Jujuboside B inhibits proliferation and induces apoptosis and ferroptosis in colorectal cancer cells with potential involvement of the MAPK signaling pathway

KE ZHAI[1], GUODONG LIU[1], CE CAO[2] and XIAOLONG WANG[2]

[1]Department of Gastroenterology, Zibo Central Hospital, Zibo, Shandong 255036, P.R. China;
[2]Department of Gastrointestinal Surgery, Zibo Central Hospital, Zibo, Shandong 255036, P.R. China

Received May 13, 2024; Accepted January 7, 2025

DOI: 10.3892/ol.2025.14908

Abstract. Colorectal cancer (CRC) is one of the most prevalent and life-threatening malignancies worldwide. Jujuboside B (JUB) is a bioactive compound derived from the seeds of *Ziziphus jujuba*, known for its potential anticancer properties. The present study aimed to investigate the association of JUB with inhibiting the proliferation, apoptosis and ferroptosis of human CRC cells with mitogen-activated protein kinase (MAPK) pathway regulation. First, the human CRC HCT116 cell line was treated with different concentrations of JUB. Subsequently, cell viability was evaluated using MTT assay and colony formation was assessed using a colony formation assay. Flow cytometry was used to detect cell apoptosis and the levels of reactive oxygen species. Western blotting was utilized to assess the expression levels of apoptosis-related proteins, ferroptosis regulators and MAPK pathway-related proteins. In addition, biochemical assay kits were used to evaluate the levels of malondialdehyde, glutathione, total iron and ferrous iron. The results demonstrated that cell viability and colony formation were markedly decreased after JUB treatment, whilst the level of apoptosis was notably increased in a concentration-dependent manner. Using electron microscopy, cells treated with JUB exhibited typical apoptotic bodies, as well as mitochondrial swelling and cristae disruption, further demonstrating JUB-induced cell apoptosis. Western blot analysis indicated that JUB treatment markedly reduced the expression of B-cell lymphoma-2 (Bcl-2) but notably increased the expression of Bcl-2 associated X-protein and cleaved caspase-3. Additionally, JUB induced ferroptosis and inhibited the MAPK signaling pathway in CRC cells. Collectively, the findings of the present study suggest that JUB has the potential to inhibit CRC cell proliferation and induce apoptosis through regulating the MAPK pathway. Therefore, JUB may be a promising therapeutic agent for the treatment of CRC.

Correspondence to: Dr Xiaolong Wang, Department of Gastrointestinal Surgery, Zibo Central Hospital, 54 Gongqingtuan Road, Zibo, Shandong 255036, P.R. China
E-mail: wxl8394@126.com

Key words: jujuboside B, colorectal cancer, cell proliferation, ferroptosis, mitogen-activated protein kinase pathway

Introduction

Currently, the main treatment modalities for colorectal cancer (CRC) include surgery, chemotherapy, radiotherapy, targeted therapy and immunotherapy. Common chemotherapy drugs include 5-fluorouracil, oxaliplatin and irinotecan (1). However, cancer cells can develop resistance to these chemotherapeutic drugs through mechanisms such as drug inactivation, alterations in drug influx and efflux and overexpression of ATP-binding cassette transport proteins (2). Radiotherapy is primarily used for locally advanced rectal cancer, with preoperative radiotherapy able to shrink tumors, increase surgical resection rates and reduce postoperative recurrence (3). Targeted therapies such as anti-EGFR (cetuximab) and anti-VEGF (bevacizumab) drugs, have demonstrated marked efficacy in the treatment of metastatic CRC (1). Previous studies have also explored new targets and combinations to enhance the specificity and effectiveness of these treatments (4,5). Immunotherapy has made notable progress in CRC, particularly with immune checkpoint inhibitors (pembrolizumab and nivolumab) showing efficacy in patients with high microsatellite instability or mismatch repair deficiency (6). Despite these treatment options, ~50% of patients with CRC still experience incurable recurrent CRC. Therefore, there is an urgent need to develop new targeted therapeutic strategies to meet the clinical needs of patients with CRC (7).

Natural products have been a notable source of several novel chemotherapeutic drugs. In previous decades, natural compounds have served a crucial role in the development of anticancer drugs, offering several active molecules with novel structures (8,9). Although natural products and their analogues, such as paclitaxel and camptothecin (10), have become indispensable in clinical practice, the treatment of CRC still faces numerous challenges. Recent studies have suggested that evodiamine may inhibit the development of CRC by modulating the gut microbiome and suppressing intestinal inflammation (10-12). Additionally, bioinformatic methods based on high-throughput DNA sequencing have identified tumor-specific

antigens associated with single nucleotide variants, offering a new strategy for the treatment of CRC (13).

Jujuboside B (JUB), a natural saponin compound, is one of the main active components of *Ziziphus jujuba* and possesses a wide range of pharmacological effects and application values. JUB exhibits multiple biological activities, including antibacterial, anti-inflammatory and antioxidant properties (13,14). Previously, JUB has been reported to induce apoptosis and demonstrate antitumor activity in several tumor types. In breast cancer, its antitumor effects are associated with the induction of apoptosis and autophagy (15). Moreover, JUB can inhibit angiogenesis and tumor growth by blocking the VEGF receptor 2 signaling pathway (16). Additionally, JUB inhibits intimal hyperplasia and vascular smooth muscle cell dedifferentiation, proliferation and migration through activating the adenosine monophosphate-activated protein kinase/peroxisome proliferator-activated receptor γ signaling (17). Despite these findings, the full antitumor potential and underlying mechanisms of JUB remain unclear.

The mitogen-activated protein kinase (MAPK) signaling pathway is closely related to several biological processes, including cell proliferation, differentiation, apoptosis and angiogenesis. Additionally, MAPK is a fundamental pathway in mammalian cells (18). Previous studies have reported that the abnormal activation of certain proteins within the MAPK pathway is associated with the occurrence and development of several cancers, such as liver cancer (19) and CRC (20). Hence, targeting proteins associated with this pathway can serve as an effective strategy for cancer treatment. However, whether JUB regulates the MAPK pathway in CRC remains to be elucidated. Therefore, the present study aimed to investigate the effects of JUB on the proliferation and apoptosis of human CRC cells, as well as its regulatory impact on the MAPK pathway.

Materials and methods

Cell culture. The CRC HCT116 cell line was purchased from the National Collection of Authenticated Cell Cultures. The cells were cultured in Roswell Park Memorial Institute 1640 medium (HyClone; Cytiva) containing 10% fetal bovine serum (HyClone; Cytiva) and 100 U/ml penicillin (HyClone; Cytiva) in an incubator at 37˚C with 5% CO_2.

Cell viability assay. An MTT assay was utilized to assess the viability of HCT116 cells treated with varying concentrations of JUB (Sigma-Aldrich; Merck KGaA). Cells in the logarithmic growth phase were seeded into a 96-well culture plate at a density of $5x10^3$ cells/well, with a total volume of 100 μl. The cells were then cultured at 37˚C for 48 h in media (Gibco) containing different concentrations of JUB (0, 5, 10, 20, 40 and 80 μM). Subsequently, the cells were incubated with MTT (5 mg/ml; Sigma-Aldrich; Merck KGaA) in the dark at 37˚C for 2 h. Subsequently, dimethyl sulfoxide (Sigma-Aldrich; Merck KGaA) was added to dissolve the formazan crystals. Finally, the optical density at 570 nm was measured using an ELx800 microplate reader (BioTek; Agilent Technologies, Inc.).

Cell colony formation assay. A colony formation assay was used to assess cell proliferation under different experimental treatments. Briefly, HCT116 cells in the logarithmic growth phase were digested, centrifuged at 300 x g for 5 min at 4˚C, resuspended and counted. Subsequently, HCT116 cells (1,000 cells/well) treated with 0, 10, 20 and 40 μM JUB were seeded in 6-well plates and cultured at 37˚C for 1 week. Once the colonies became visible to the naked eye, the plates were taken out and the medium was discarded. After rinsing with phosphate buffered saline (PBS), the cells were fixed with 4% paraformaldehyde (Sigma-Aldrich; Merck KGaA) at room temperature for 20 min. The paraformaldehyde was then discarded and the cells were stained with 0.1% crystal violet (Sigma-Aldrich; Merck KGaA) at room temperature for 3 min. Upon washing off the crystal violet, visible cell clusters containing at least 50 cells were captured and counted using a light microscope (Nikon Corporation) and manually counted.

Flow cytometry. HCT116 cells were seeded in 6-well plates at a density of $4x10^5$ cells/well and treated with varying concentrations of JUB (0, 10, 20 and 40 μM). After 48 h, the cells were harvested using trypsin and washed twice with PBS before being collected into Eppendorf tubes. The treated cells were then resuspended using 195 μl Annexin V-Fluorescein isothiocyanate binding solution (Beyotime Institute of Biotechnology). Subsequently, 5 μl Annexin V-Fluorescein isothiocyanate and 10 μl propidium iodide (Thermo Fisher Scientific, Inc.) staining solution were added, followed by gentle agitation of the mixture. The cells were then incubated in the dark at room temperature (20-25˚C) for 10-20 min. After adding 400 μl binding buffer, the cells were analyzed using an LSRFortessa™ flow cytometer (BD Biosciences).

Transmission electron microscopy (TEM). After exposing the human CRC HCT116 cell line to different concentrations of JUB (0, 10, 20 and 40 μM) for 24 h, the samples were fixed overnight at 4˚C in 2.5% glutaraldehyde (v/v) in 0.1 M PBS buffer, followed by post-fixation with 1% osmium tetroxide in the same buffer at 4˚C for 2 h. The samples were then dehydrated in graded ethanol series (30, 50, 70, 90, and 100%) at room temperature for 15 min each, followed by dehydration in ethanol/epoxy resin gradients (3:1, 1:1, 1:3 and 0:1) at room temperature for 15 min each before embedding in epoxy resin for 12 h. Ultrathin sections (60-80 nm) were prepared using an ultramicrotome, stained with 3% uranyl acetate and lead citrate and observed under a transmission electron microscope to analyze the ultrastructural changes in the cells.

Western blot. Total proteins were extracted from the cells using radioimmunoprecipitation assay lysis buffer (cat. no. 89900; Thermo Fisher Scientific, Inc.) and protein concentration was determined using a bicinchoninic acid assay. Subsequently, 10 μg protein/lane and subjected to 10-12% sodium dodecyl sulfate-polyacrylamide gel electrophoresis for 120 min, transferred to a polyvinylidene fluoride membrane (cat. no. LC2005; Thermo Fisher Scientific, Inc.) using a wet transfer method, and then blocked with 5% skimmed milk at room temperature for 2 h. Primary antibodies were applied overnight incubation at 4˚C. The primary antibodies (all Abcam) were as follows: Anti-B-cell lymphoma-2 (Bcl-2, 1:1,000, ab241548), anti-Bcl-2 associated X-protein (Bax, 1:1,000, ab3191), anti-cleaved caspase-3 (1:1,000, ab2302), anti-caspase-3 (1:1,000, ab184787), anti-solute carrier family

7 member 11 (SLC7A11, 1:1,000, ab307601), anti-glutathione peroxidase 4 (GPX4, 1:1,000, ab252833), anti-acyl-CoA synthetase long chain family member 4 (ACSL4, 1:1,000, ab155282), anti-transferrin receptor 1 (TFR1, 1:1,000, ab214039), anti-MAPK kinase (MEK, 1:1,000, ab265586), anti-phosphorylated (p)-MEK (1:1,000; cat. no. ab307509), anti-p-extracellular signal-regulated kinase (ERK, 1:1,000, ab32537), anti-p-ERK (1:1,000, ab201015) and anti-GAPDH, 1:1,000, ab8245, Abcam). After washing three times with tris buffered saline with 0.1% Tween 20 (TBST), the membrane was incubated with HRP-conjugated goat anti-rabbit IgG (1:1,000, ab181662, Abcam) or anti-mouse IgG (1:1,000; cat. no. ab181662, Abcam) for 2 h. After three additional washes with TBST, the protein bands were visualized using electrochemiluminescence (MilliporeSigma; KGaA) and recorded with a ChemiDoc EQ System (Bio-Rad Laboratories, Inc.). The grayscale intensity of the bands was analyzed using ImageJ software (version 1.53t, National Institutes of Health).

Measurement of reactive oxygen species (ROS). Cell suspensions were seeded into 6-well plates at a density of $2x10^5$ cells per well. After receiving 0 μM (control group) and 40 μM JUB (JUB group) treatment for 48 h at 37˚C, HCT116 cells were pretreated with 1 μM ferrostatin-1 (Fer-1), a ferroptosis inhibitor (Selleck Chemicals) at 37˚C for 2 h. Subsequently, the cells were treated with 40 μM JUB for another at 37˚C 48 h, constituting the JUB + Fer-1 group. Intracellular ROS levels were then measured using flow cytometry using the oxidation-activated fluorescent dye DCHF-DA (Beyotime Institute of Biotechnology). Briefly, cell samples were incubated with PBS containing 10 μM DCHF-DA at 37˚C for 20 min. The cells were then washed three times with PBS, digested with trypsin and washed twice with cold PBS. Lastly, the ROS levels were detected using an LSRFortessa™ flow cytometer (BD Biosciences). Flow cytometry data were analyzed using FlowJo software (version X.0.7, BD Biosciences).

Detection of malondialdehyde (MDA), glutathione (GSH), total iron and ferrous iron (Fe^{2+}) levels. The levels of MDA, glutathione GSH, total iron and Fe^{2+} in HCT116 cells of the control, JUB and JUB + Fer-1 groups were determined using the Lipid Peroxidation Assay Kit, GSH Colorimetric Assay Kit (cat. no. A006-2), Total Iron Colorimetric Assay Kit (A040) and Ferrous Iron Colorimetric Assay Kit (A039-2), respectively (all Nanjing Jiancheng Bioengineering Institute). The specific detection steps were followed according to the manufacturer's protocols.

Statistical analysis. SPSS 19.0 (IBM Corp.) was used for data analysis and data plotting was performed using GraphPad Prism 9.0 (Dotmatics). All values are expressed as mean ± standard deviation. A one-way analysis of variance was performed, followed by a Tukey's HSD post hoc test. $P<0.05$ was considered to indicate a statistically significant difference.

Results

Effect of JUB on the viability and proliferation of human CRC cells. To assess the hypothesis that JUB may have anticancer activity, the effect of JUB on the viability of human CRC HCT116 cells was assessed. The results of the MTT assay demonstrated that, compared with the 0 μM group, the survival rate of HCT116 cells was significantly decreased in the 5, 10, 20, 40 and 80 μM groups (all $P<0.01$), indicating that JUB had an inhibitory effect on the viability of HCT116 cells in a concentration-dependent manner (Fig. 1A). The colony formation assay results demonstrated that the colony formation of HCT116 cells was significantly reduced in the 10, 20 and 40 μM groups (all $P<0.01$) in a concentration-dependent manner compared with the 0 μM group (Fig. 1B and C). These results suggested that JUB could inhibit the viability and proliferation of human CRC cells.

Ultrastructural changes induced by JUB in promoting apoptosis of HCT-116 cells. High-magnification TEM demonstrated that different concentrations of JUB induced marked effects on the endoplasmic reticulum (ER) and mitochondrial structures in HCT-116 cells (Fig. 1D). In the 0 μM JUB control group, the ER in HCT-116 cells was neatly arranged with ribosomes attached and the mitochondria were abundant and structurally intact, with clearly visible cristae. As the concentration of JUB increased, the 10 μM treatment group showed that the rough ER exhibited degranulation, free ribosomes increased and certain mitochondria became vacuolated. In the 20 μM treatment group, the vacuolation of mitochondria increased, autophagosomes formed and the ER expanded. In the 40 μM treatment group, cells exhibited pronounced autophagic flux, notable mitochondrial swelling, cristae fragmentation or loss and chromatin condensation with evident marginalization. These results indicate that JUB induces concentration-dependent damage to the ER and mitochondrial structures in HCT-116 cells, with high concentrations of JUB promoting autophagy and apoptosis-related ultrastructural changes.

Effects of JUB on the apoptosis of HCT116 cells. The results of the MTT and colony formation assays suggested that JUB had an antitumor effect, prompting further investigation into the underlying mechanisms of JUB. It was uncertain whether the decreased viability of tumor cells with JUB treatment was primarily due to apoptosis mechanisms or cell-cycle dysregulation. Therefore, the rate of apoptosis of HCT116 cells treated with different concentrations of JUB was evaluated. The apoptosis rate of HCT116 cells was significantly increased in the 10, 20 and 40 μM groups compared with the 0 μM group (all $P<0.01$), with higher concentrations associated with higher apoptosis rates (Fig. 2A).

To further assess the effect of JUB on cell apoptosis, the protein expression levels of three apoptotic biomarkers in cells treated with different concentrations were evaluated by western blotting. The protein expression level of Bcl-2 was significantly decreased, whilst the protein expression levels of Bax and the ratio of cleaved caspase-3/caspase-3 were significantly increased in the 10, 20 and 40 μM groups compared with the 0 μM group, in a concentration-dependent manner (Fig. 2B; all $P<0.01$). These results indicate that JUB promotes apoptosis in HCT116 cells.

JUB induces apoptosis and ferroptosis in CRC cells. Subsequently, the role of JUB (40 μM) in the ferroptosis process in HCT116 cells was assessed. The results

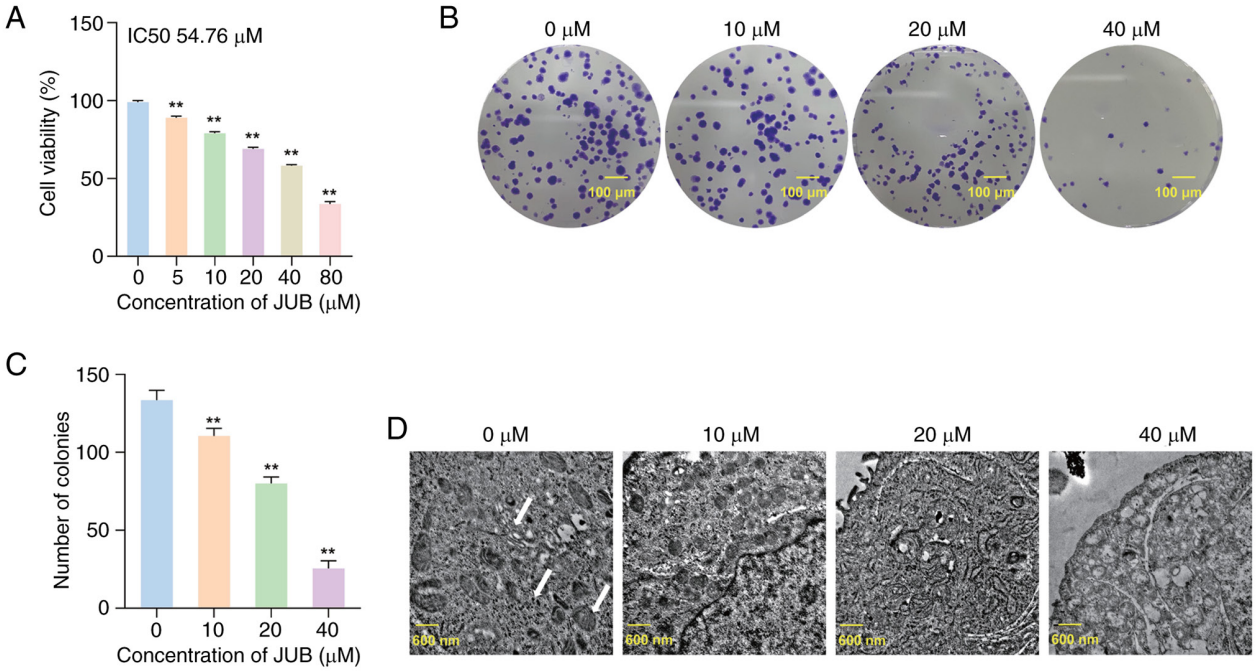

Figure 1. JUB inhibits the proliferation of HCT116 cells. (A) MTT assay was used to assess the viability of HCT116 cells treated with 0, 5, 10, 20, 40 and 80 μM JUB. (B) Colony formation assay and (C) quantification was performed to evaluate the colony formation of HCT116 cells treated with JUB. (D) Electron microscopy images showing the formation of apoptotic bodies in HCT116 cells treated with 0, 10, 20 and 40 μM JUB. **P<0.01 vs. 0 μM JUB. JUB, Jujuboside B.

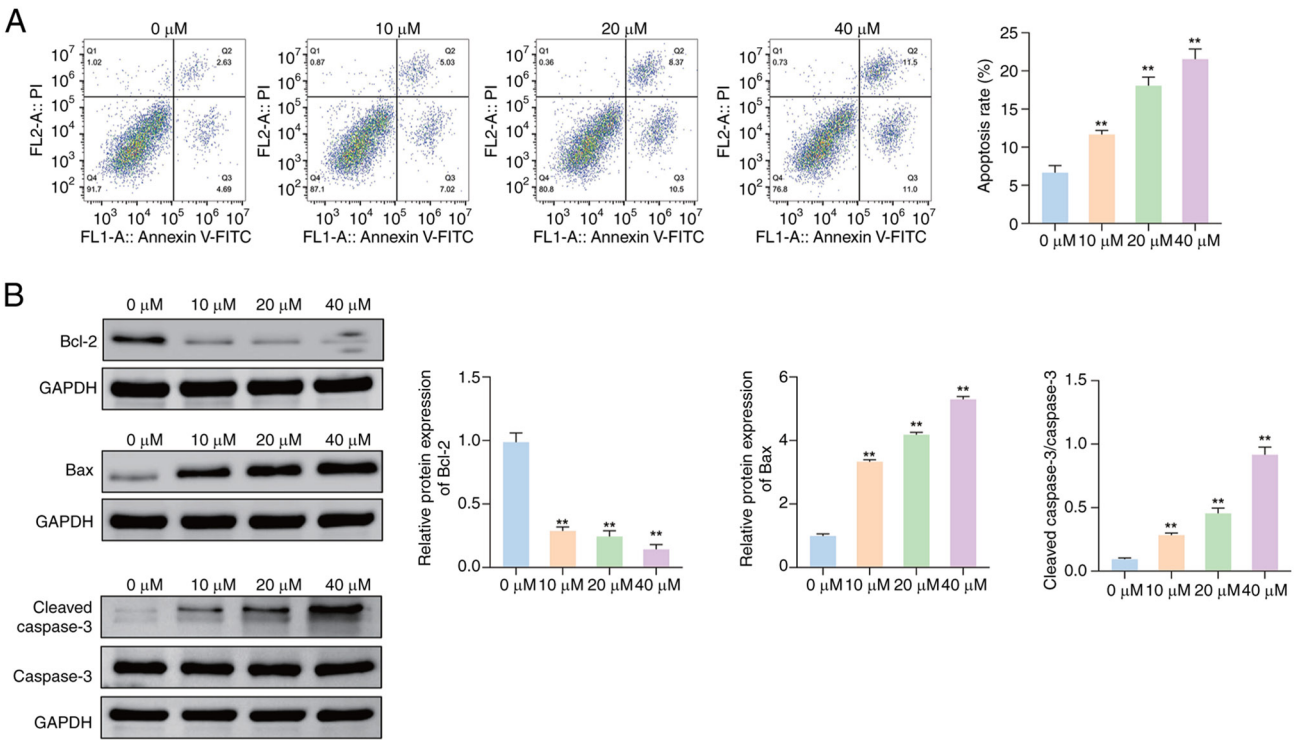

Figure 2. JUB promotes apoptosis in HCT116 cells. (A) Flow cytometry was performed to assess apoptosis of HCT116 cells treated with 0, 10, 20 and 40 μM JUB. (B) Western blotting was used to evaluate the protein expression levels of Bcl-2, Bax and cleaved caspase-3/caspase-3 in HCT116 cells treated with 0, 10, 20 and 40 μM JUB. **P<0.01 vs. 0 μM. JUB, Jujuboside B; Bcl-2, B-cell lymphoma-2; Bax, B-cell lymphoma-2 associated X-protein.

demonstrated that the ROS levels of HCT116 cells were significantly increased in the JUB group compared with the control group (Fig. 3A and B; P<0.01) and the JUB + Fer-1 group showed a significant reduction in ROS levels compared with the JUB group (P<0.01). Additionally, the levels of MDA, total iron and Fe^{2+} were significantly increased in the JUB group compared with the control group, whilst the GSH levels were significantly decreased (Fig. 3C-F; all P<0.01). The JUB

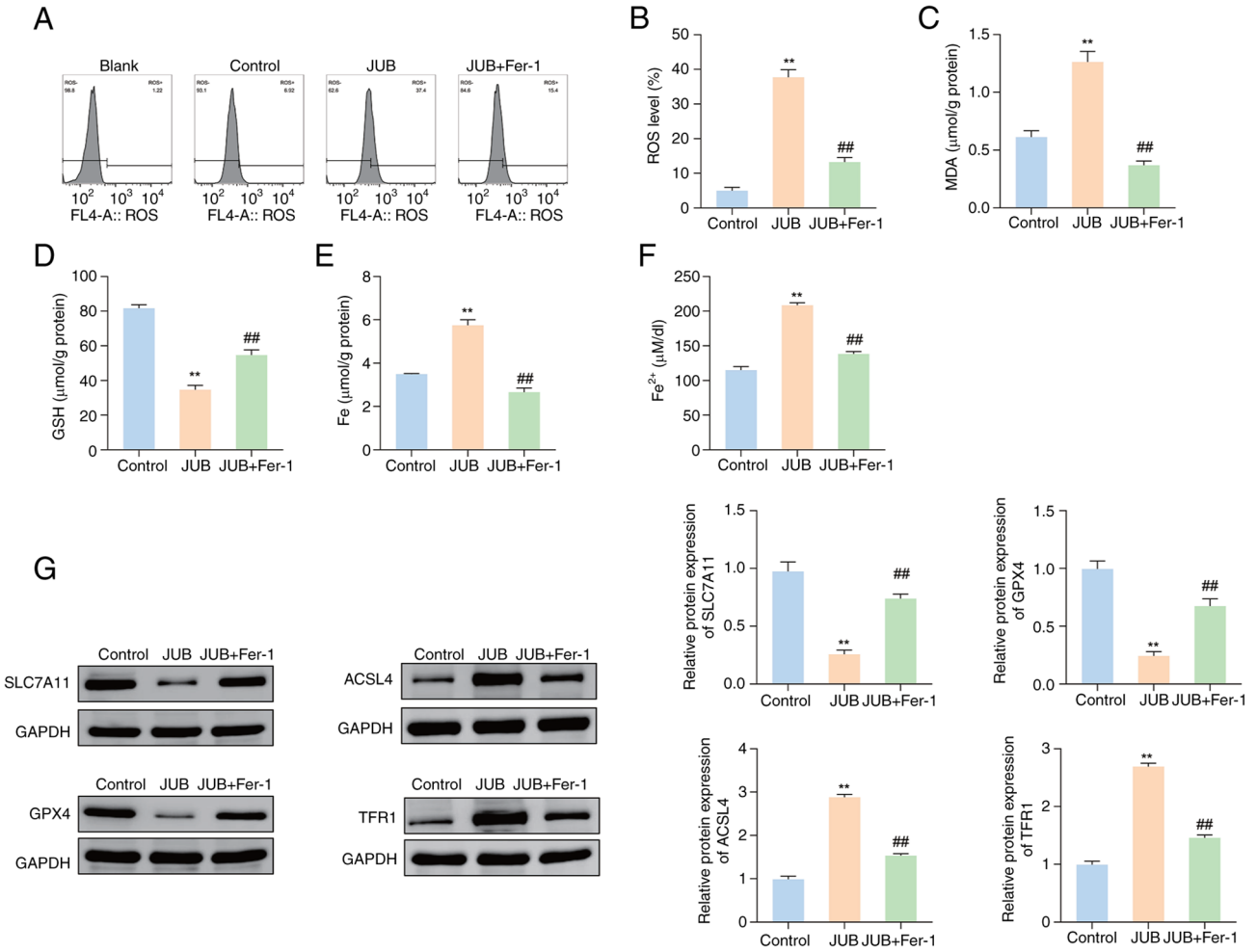

Figure 3. JUB induces ferroptosis in HCT116 cells. For the JUB + Fer-1 group, HCT116 cells were pre-treated with 1 μM Fer-1 (ferroptosis inhibitor) for 2 h, followed by treatment with 40 μM JUB for 48 h. (A) Levels of ROS in HCT116 cells of each group were assessed by flow cytometry and (B) subsequent quantification. Detection of (C) MDA and (D) GSH levels was performed. (E) Total iron level in HCT116 cells was determined using an iron assay kit. (F) Fe^{2+} level in HCT116 cells was assessed using a Fe^{2+} assay kit. (G) Western blotting was performed to analyze the protein expression levels of SLC7A11, GPX4, ACSL4 and TFR1. **P<0.01 vs. control; $^{\#\#}$P<0.01 vs. JUB. JUB, Jujuboside B; Fer-1, ferrostatin-1; ROS, reactive oxygen species; MDA, malondialdehyde; GSH, glutathione; SLC7A11, solute carrier family 7 member 11; GPX4, glutathione peroxidase 4; ACSL4, acyl-CoA synthetase long chain family member 4; TFR1, transferrin receptor 1; Fe^{2+}, ferrous iron.

+ Fer-1 group showed a significant decrease in MDA, total iron and Fe^{2+} levels, coupled with a significant increase in GSH levels compared with the JUB group (all P<0.01).

To further evaluate the role of JUB in the ferroptosis process, the expression of four ferroptosis regulatory factors (SLC7A11, GPX4, ACSL4 and TFR1) in different treatment groups was assessed. The protein expression levels of SLC7A11 and GPX4 were significantly downregulated in the JUB group compared with the control group, whilst the protein expression levels of ACSL4 and TFR1 proteins were significantly upregulated (Fig. 3G; all P<0.01). In comparison with the JUB group, the JUB + Fer-1 group demonstrated a significant increase in the protein expression of SLC7A11 and GPX4, and a decrease in the expression of ACSL4 and TFR1 (Fig. 3G; all P<0.01). These results indicate that JUB could induce ferroptosis in HCT116 cells.

Effect of JUB on the expression of MAPK pathway-related proteins in HCT116 cells. Western blot analysis demonstrated a marked reduction in the protein expression levels of p-MEK and p-ERK in HCT116 cells treated with several concentrations of JUB, compared with the 0 μM group (Fig. 4A). There were no marked differences in the protein expression levels of total MEK and ERK between the 0 μM group and other treatment groups. JUB treatment at all concentrations significantly decreased the ratios of p-MEK/MEK and p-ERK/ERK compared with the 0 μM control group, in a concentration-dependent manner (Fig. 4B; all P<0.01). These results suggest JUB could inhibit the MAPK signaling pathway in HCT116 cells.

Discussion

As reported in previous studies, Bcl-2 is a common anti-apoptotic protein in cells, whilst Bax and cleaved caspase-3 are pro-apoptotic proteins. Such proteins are considered the most important oncoproteins in apoptosis research (21,22). In the present study, HCT116 cells were treated with different concentrations of JUB. The results of the present study demonstrated that cell viability and colony formation

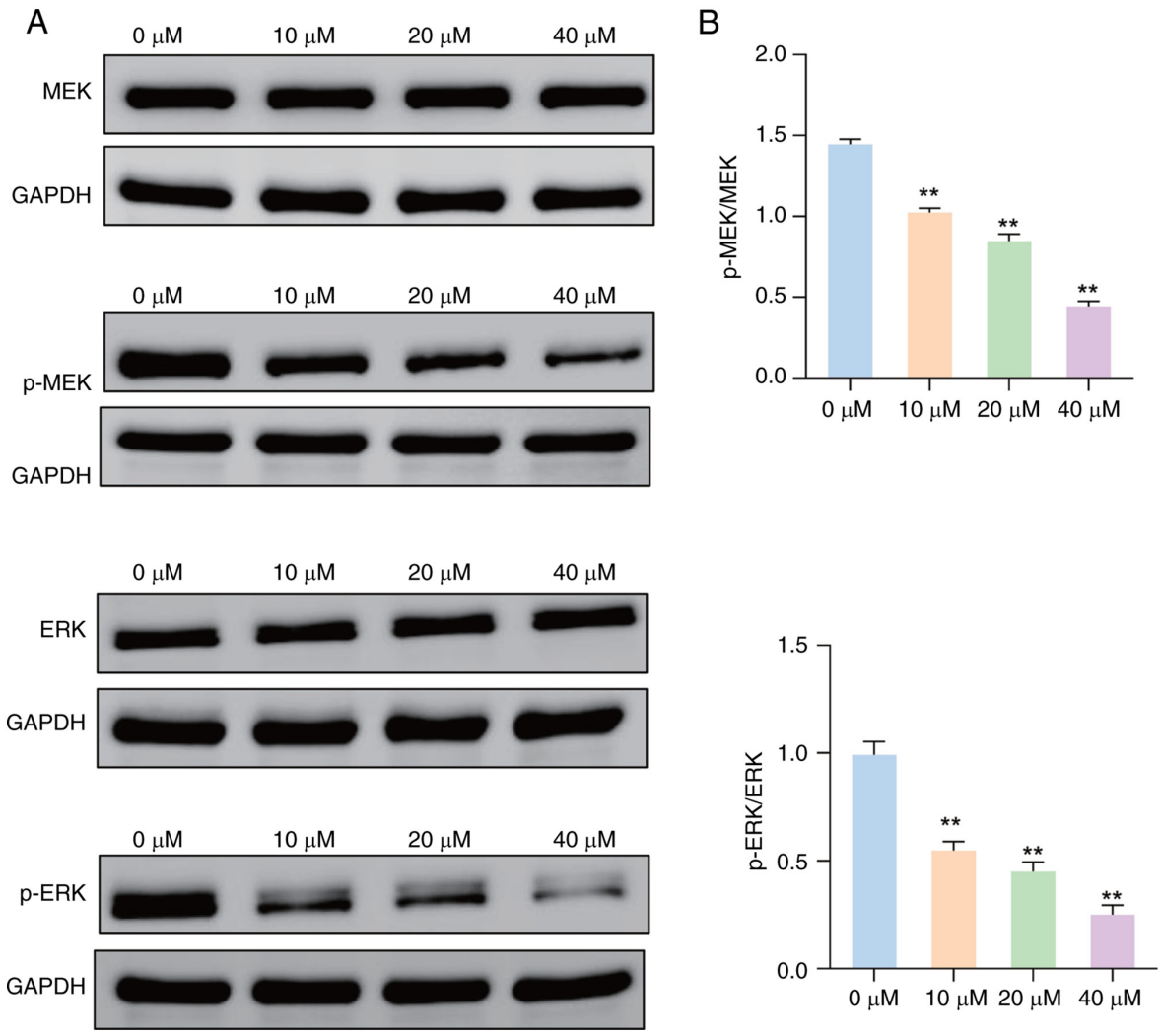

Figure 4. Effect of JUB on the expression of MAPK pathway-related proteins in HCT116 cells. (A) Western blotting was performed to assess the levels of MEK, p-MEK, ERK and p-ERK proteins in HCT116 cells treated with 0, 10, 20 and 40 μM JUB. (B) Ratios of p-MEK/MEK and p-ERK/ERK were measured in HCT116 cells after treatment with 0, 10, 20 and 40 μM JUB. **P<0.01 vs. control. JUB, Jujuboside B; MAPK, mitogen-activated protein kinase; MEK, MAPK kinase; p-MEK, phosphorylated-MEK; ERK, extracellular signal-regulated kinase; p-ERK, phosphorylated-ERK.

were significantly decreased after JUB treatment, whilst the apoptosis level was notably increased, both in a concentration-dependent manner. Western blot analysis indicated that JUB treatment significantly reduced the expression of Bcl-2, whilst increasing the expression of Bax and the ratio of cleaved caspase-3/caspase-3. Additionally, TEM revealed marked ultrastructural changes in the treated cells, including chromatin marginalization, cell membrane blebbing, apoptotic body formation, as well as mitochondrial swelling and cristae disruption or loss. Therefore, the results of the present study suggest that JUB has anti-CRC effects.

Ferroptosis, a novel form of cell death, possesses a unique mechanism and can be specifically identified by the accumulation of Fe^{2+} and the increase in lipid peroxidation, particularly polyunsaturated fatty acids (23). Ferroptosis has been reported to be associated with the occurrence and treatment of several diseases such as Alzheimer's and Parkinson's, ischemia-reperfusion injury, liver fibrosis (24). In addition, a growing body of evidence indicates that ferroptosis is involved in the occurrence, progression and suppression of tumors. Ferroptosis suppresses tumors by inducing cell death through lipid peroxidation and iron metabolism disruption, regulated by factors like p53. However, in some cases, cancer cells can resist ferroptosis, allowing them to evade oxidative stress and promote tumor progression, especially in the tumor microenvironment (25). In cancer therapy, many clinical chemotherapeutic agents not only initiate apoptosis, but also induce ferroptosis and prevent cancer growth (26,27). In the present study, the inclusion of the Fer-1 treatment group aimed to further assess the specificity of JUB-induced cell death. Fer-1 is a well-known ferroptosis inhibitor that effectively inhibits the ferroptosis process. By pre-treating cells with Fer-1 followed by JUB treatment, significant decreases in the protein expression levels of ferroptosis-related markers were observed. These results indicated that the cell death induced by JUB occurs through the ferroptosis pathway.

In the present study, the effect of JUB on the expression levels of key ferroptosis markers was explored in HCT116 cells by treatment with Fer-1. Iron metabolism in the ferroptosis process can cause the accumulation of ROS. The increase in intracellular ROS can lead to mitochondrial DNA strand breaks and DNA degradation, thereby resulting in apoptosis (28). The

changes in GSH synthesis and MDA levels are also indicators of ferroptosis-associated lipid peroxidation (29,30). MDA, one of the products of lipid peroxidation, is positively associated with ferroptosis, whilst the association between GSH and ferroptosis is negative (31). The change in iron content is a notable characteristic of ferroptosis. The accumulation of Fe^{2+} can specifically elevate oxidative stress levels, demonstrating a positive association with ferroptosis (32). The present study demonstrated that, compared with the control group, JUB treatment significantly increased the levels of ROS, MDA, total iron and Fe^{2+} in HCT116 cells, whilst markedly decreasing the GSH level. However, after the addition of the ferroptosis inhibitor Fer-1, the levels of ROS, MDA, total iron and Fe^{2+} were significantly reduced compared with the JUB group, whilst the GSH level was markedly increased. These results demonstrate that JUB could induce ferroptosis.

SLC7A11 is a specific type of amino acid transporter, particularly for glutamate and cystine (33). The primary function of SLC7A11 is inhibition of ferroptosis in cells (34). GPX4 inhibits lipid peroxidation, thereby protecting cells from oxidative damage and the upregulation of GPX4 can inhibit ferroptosis (35). Decreased expression of ACSL4 can reduce the accumulation of lipid peroxidation substrates in cells, thereby inhibiting ferroptosis (36). TFR1 serves a crucial role in regulating cellular iron metabolism and maintaining iron balance, and acts as a specific marker of ferroptosis (37). The results of the present study demonstrated JUB treatment significantly downregulated the expression levels of SLC7A11 and GPX4 proteins, whilst markedly upregulating the levels of ACSL4 and TFR1. However, the combination of JUB and Fer-1 significantly increased the expression of SLC7A11 and GPX4 but inhibited the expression of ACSL4 and TFR1. The aforementioned findings suggest that JUB may promote ferroptosis in HCT116 cells by affecting the expression of SLC7A11, GPX4, ACSL4 and TFR1. JUB treatment appears to downregulate the expression of SLC7A11 and GPX4, both of which are key regulators of cellular antioxidant defense, thereby decreasing the ability to counteract oxidative stress. In contrast, JUB treatment upregulates the expression of ACSL4 and TFR1, proteins involved in lipid peroxidation and iron homeostasis, respectively. These changes in protein expression may enhance lipid peroxidation and increase intracellular iron levels, contributing to the induction of ferroptosis.

The MAPK pathway, consisting of ERK1/2, MEK1/2 and p38 (38), is one of the most commonly mutated oncogenic pathways in several cancers (39), including colorectal cancer, lung cancer, and thyroid cancer. The abnormal activation of proteins such as EGFR, RAS (including KRAS, HRAS, NRAS), and RAF (such as BRAF) can lead to MAPK pathway dysregulation, resulting in uncontrolled cellular proliferation and dedifferentiation (40). In colorectal cancer, the MAPK pathway is generally activated, contributing to the development, progression, and resistance to therapy (41). In the present study, JUB significantly reduced the levels of p-MEK and p-ERK proteins, as well as the ratios of p-MEK/MEK and p-ERK/ERK, in HCT116 cells, indicating that JUB inhibits MAPK pathway activation. These findings suggest that the inhibitory effect of JUB on the MAPK pathway may play a role in reducing CRC cell proliferation, colony formation, and survival, potentially contributing to its overall anticancer effects. Alternatively, the anticancer effects of JUB may be primarily mediated through the induction of ferroptosis or cell death, rather than solely through MAPK pathway inhibition. Further studies are required to determine the relative contributions of ferroptosis induction and MAPK pathway inhibition to the observed effects of JUB treatment in CRC cells.

Although the antitumor activity of JUB has been reported in other types of cancer, the present study is the first to systematically investigate the mechanism of JUB in CRC, to the best of our knowledge. Not only were the effects of JUB on the proliferation and apoptosis of HCT116 cells evaluated, but also its specific molecular mechanisms by regulating the MAPK signaling pathway and inducing ferroptosis were explored. The present study is also the first to reveal that the JUB inhibits proliferation, colony formation, and induces apoptosis and ferroptosis in CRC cells, to the best of our knowledge.

However, the present study has certain limitations, such as the lack of animal experiments and the lack of experiments demonstrating the expression changes of four ferroptosis regulatory factors (SLC7A11, GPX4, ACSL4 and TFR1) under normal ferroptotic conditions as a control. Future research should evaluate of the impact of JUB on normal tissues, and its dose toxicity and safety, through *both in vitro* cell experiments on different cell lines and *in vivo* animal models. Additionally, incorporating both MAPK inhibitors and activators would provide more insight into the mechanisms by which JUB affects the MAPK pathway. Activating the MAPK pathway during JUB treatment would help confirm whether the effects of JUB on proliferation, apoptosis, and ferroptosis are mediated through this pathway. Only detecting activation of the MAPK pathway does not provide evidence that the mechanism of JUB is mediated by the MAPK pathway. However, the present study demonstrate that JUB inhibits the MAPK pathway by reducing the phosphorylation levels of MEK and ERK in HCT116 cells. The antitumor effects of JUB on different types of tumors should also be investigated, validating its anticancer activity both *in vitro* and *in vivo*. Given the varied role of the MAPK pathway, the impact of JUB on other biological processes dependent on this pathway should be studied to ensure its safety and specificity in cancer treatment.

In summary, the results of the present study demonstrated that JUB can inhibit the proliferation of CRC cells and promote apoptosis and ferroptosis. The inhibition of the MAPK pathway suggests that the effects of JUB on apoptosis and ferroptosis may be related to the regulation of this pathway. However, further studies are needed to confirm this association.

Acknowledgements

Not applicable.

Funding

No funding was received.

Availability of data and materials

The data generated in the present study may be requested from the corresponding author.

Authors' contributions

KZ and XW conceived and designed the study. KZ and XW performed the experiments. GL and CC contributed to data acquisition. GL and CC analyzed the data. GL and CC interpreted the data. KZ and GL confirm the authenticity of all the raw data. GL and CC edited the manuscript draft. KZ and XW reviewed and edited the manuscript. All authors have read and approved the final manuscript.

Ethics approval and consent to participate

Not applicable.

Patient consent for publication

Not applicable.

Competing interests

The authors declare that they have no competing interests.

References

1. Eng C, Jácome AA, Agarwal R, Hayat MH, Byndloss MX, Holowatyj AN, Bailey C and Lieu CH: A comprehensive framework for early-onset colorectal cancer research. Lancet Oncol 23: e116-e128, 2022.
2. Zhou J, Ji Q and Li Q: Resistance to anti-EGFR therapies in metastatic colorectal cancer: Underlying mechanisms and reversal strategies. J Exp Clin Cancer Res 40: 328, 2021.
3. Zhong Y, Chen X, Wu S, Fang H, Hong L, Shao L, Wang L and Wu J: Deciphering colorectal cancer radioresistance and immune microrenvironment: Unraveling the role of EIF5A through single-cell RNA sequencing and machine learning. Front Immunol 15: 1466226, 2024.
4. Li QH, Wang YZ, Tu J, Liu CW, Yuan YJ, Lin R, He WL, Cai SR, He YL and Ye JN: Anti-EGFR therapy in metastatic colorectal cancer: Mechanisms and potential regimens of drug resistance. Gastroenterol Rep (Oxf) 8: 179-191, 2020.
5. Zhang Q, Zheng Y, Liu J, Tang X, Wang Y, Li X, Li H, Zhou X, Tang S, Tang Y, *et al*: CircIFNGR2 enhances proliferation and migration of CRC and induces cetuximab resistance by indirectly targeting KRAS via sponging to MiR-30b. Cell Death Dis 14: 24, 2023.
6. Siegel RL, Wagle NS, Cercek A, Smith RA and Jemal A: Colorectal cancer statistics, 2023. CA Cancer J Clin 73: 233-254, 2023.
7. Xia C, Dong X, Li H, Cao M, Sun D, He S, Yang F, Yan X, Zhang S, Li N and Chen W: Cancer statistics in China and United States, 2022: Profiles, trends, and determinants. Chin Med J (Engl) 135: 584-590, 2022.
8. Kashiwagi S, Asano Y, Goto W, Takada K, Takahashi K, Hatano T, Tanaka S, Takashima T, Tomita S, Motomura H, *et al*: Mesenchymal-epithelial transition and tumor vascular remodeling in eribulin chemotherapy for breast cancer. Anticancer Res 38: 401-410, 2018.
9. Miyamoto M, Takano M, Kuwahara M, Soyama H, Kato K, Matuura H, Sakamoto T, Takasaki K, Aoyama T, Yoshikawa T and Furuya K: Efficacy of combination chemotherapy using irinotecan and nedaplatin for patients with recurrent and refractory endometrial carcinomas: Preliminary analysis and literature review. Cancer Chemother Pharmacol 81: 111-117, 2018.
10. Zhu LQ, Zhang L, Zhang J, Chang GL, Liu G, Yu DD, Yu XM, Zhao MS and Ye B: Evodiamine inhibits high-fat diet-induced colitis-associated cancer in mice through regulating the gut microbiota. J Integr Med 19: 56-65, 2021.
11. Morazán-Fernández D, Mora J and Molina-Mora JA: In silico pipeline to identify tumor-specific antigens for cancer immunotherapy using exome sequencing data. Phenomics 3: 130-137, 2023.
12. Wang M, Zhou B, Cong W, Zhang M, Li Z, Li Y, Liang S, Chen K, Yang D and Wu Z: Amelioration of AOM/DSS-Induced murine colitis-associated cancer by evodiamine intervention is primarily associated with gut microbiota-metabolism-inflammatory signaling axis. Front Pharmacol 12: 797605, 2021.
13. Lee IC and Bae JS: Hepatic protective effects of jujuboside B through the modulation of inflammatory pathways. Biotechnology and Bioprocess Engineering 27: 336-343, 2022.
14. Molagoda IMN, Lee KT, Athapaththu A, Choi YH, Hwang J, Sim SJ, Kang S and Kim GY: Flavonoid glycosides from ziziphus jujuba var. inermis (Bunge) rehder seeds inhibit alpha-melanocyte-stimulating hormone-mediated melanogenesis. Int J Mol Sci 22: 7701, 2021.
15. Guo L, Liang Y, Wang S, Li L, Cai L, Heng Y, Yang J, Jin X, Zhang J, Yuan S, *et al*: Jujuboside B inhibits the proliferation of breast cancer cell lines by inducing apoptosis and autophagy. Front Pharmacol 12: 668887, 2021.
16. Zhang P, Lai X, Zhu MH, Shi J, Pan H, Huang Y, Guo RJ, Lu Q, Fang C and Zhao M: Jujuboside B suppresses angiogenesis and tumor growth via blocking VEGFR2 signaling pathway. Heliyon 9: e17072, 2023.
17. Ji Z, Li J and Wang J: Jujuboside B inhibits neointimal hyperplasia and prevents vascular smooth muscle cell dedifferentiation, proliferation, and migration via activation of AMPK/PPAR-γ signaling. Front Pharmacol 12: 672150, 2021.
18. Kim EK and Choi EJ: Pathological roles of MAPK signaling pathways in human diseases. Biochim Biophys Acta 1802: 396-405, 2010.
19. Moon H and Ro SW: MAPK/ERK signaling pathway in hepatocellular carcinoma. Cancers (Basel) 13: 3026, 2021.
20. Pashirzad M, Khorasanian R, Fard MM, Arjmand MH, Langari H, Khazaei M, Soleimanpour S, Rezayi M, Ferns GA, Hassanian SM and Avan A: The therapeutic potential of MAPK/ERK inhibitors in the treatment of colorectal cancer. Curr Cancer Drug Targets 21: 932-943, 2021.
21. Liu G, Wang T, Wang T, Song J and Zhou Z: Effects of apoptosis-related proteins caspase-3, Bax and Bcl-2 on cerebral ischemia rats. Biomed Rep 1: 861-867, 2013.
22. Dolka I, Krol M and Sapierzynski R: Evaluation of apoptosis-associated protein (Bcl-2, Bax, cleaved caspase-3 and p53) expression in canine mammary tumors: An immunohistochemical and prognostic study. Res Vet Sci 105: 124-133, 2016.
23. Xie Y, Hou W, Song X, Yu Y, Huang J, Sun X, Kang R and Tang D: Ferroptosis: Process and function. Cell Death Differ 23: 369-379, 2016.
24. Jiang X, Stockwell BR and Conrad M: Ferroptosis: Mechanisms, biology and role in disease. Nat Rev Mol Cell Biol 22: 266-282, 2021.
25. Wang Y, Wei Z, Pan K, Li J and Chen Q: The function and mechanism of ferroptosis in cancer. Apoptosis 25: 786-798, 2020.
26. Lachaier E, Louandre C, Godin C, Saidak Z, Baert M, Diouf M, Chauffert B and Galmiche A: Sorafenib induces ferroptosis in human cancer cell lines originating from different solid tumors. Anticancer Res 34: 6417-6422, 2014.
27. Yang R, Li Y, Wang X, Yan J, Pan D, Xu Y, Wang L and Yang M: Doxorubicin loaded ferritin nanoparticles for ferroptosis enhanced targeted killing of cancer cells. RSC Adv 9: 28548-28553, 2019.
28. Zhang J, Wang X, Vikash V, Ye Q, Wu D, Liu Y and Dong W: ROS and ROS-mediated cellular signaling. Oxid Med Cell Longev 2016: 4350965, 2016.
29. Cao JY and Dixon SJ: Mechanisms of ferroptosis. Cell Mol Life Sci 73: 2195-2209, 2016.
30. Tang D and Kroemer G: Ferroptosis. Curr Biol 30: R1292-R1297, 2020.
31. Wang B, Wang Y, Zhang J, Hu C, Jiang J, Li Y and Peng Z: ROS-induced lipid peroxidation modulates cell death outcome: Mechanisms behind apoptosis, autophagy, and ferroptosis. Arch Toxicol 97: 1439-1451, 2023.
32. Li Y, Du Y, Zhou Y, Chen Q, Luo Z, Ren Y, Chen X and Chen G: Iron and copper: Critical executioners of ferroptosis, cuproptosis and other forms of cell death. Cell Commun Signal 21: 327, 2023.
33. Koppula P, Zhang Y, Zhuang L and Gan B: Amino acid transporter SLC7A11/xCT at the crossroads of regulating redox homeostasis and nutrient dependency of cancer. Cancer Commun (Lond) 38: 12, 2018.
34. Iida Y, Okamoto-Katsuyama M, Maruoka S, Mizumura K, Shimizu T, Shikano S, Hikichi M, Takahashi M, Tsuya K, Okamoto S, *et al*: Effective ferroptotic small-cell lung cancer cell death from SLC7A11 inhibition by sulforaphane. Oncol Lett 21: 71, 2021.
35. Seibt TM, Proneth B and Conrad M: Role of GPX4 in ferroptosis and its pharmacological implication. Free Radic Biol Med 133: 144-152, 2019.

36. Doll S, Proneth B, Tyurina YY, Panzilius E, Kobayashi S, Ingold I, Irmler M, Beckers J, Aichler M, Walch A, *et al*: ACSL4 dictates ferroptosis sensitivity by shaping cellular lipid composition. Nat Chem Biol 13: 91-98, 2017.
37. Feng H, Schorpp K, Jin J, Yozwiak CE, Hoffstrom BG, Decker AM, Rajbhandari P, Stokes ME, Bender HG, Csuka JM, *et al*: Transferrin receptor is a specific ferroptosis marker. Cell Rep 30: 3411-3423 e3417, 2020.
38. Sun Y, Liu WZ, Liu T, Feng X, Yang N and Zhou HF: Signaling pathway of MAPK/ERK in cell proliferation, differentiation, migration, senescence and apoptosis. J Recept Signal Transduct Res 35: 600-604, 2015.
39. Liu YC, Lin TJ, Chong KY, Chen GY, Kuo CY, Lin YY, Chang CW, Hsiao TF, Wang CL, Shih YC and Yu CJ: Targeting the ERK1/2 and p38 MAPK pathways attenuates Golgi tethering factor golgin-97 depletion-induced cancer progression in breast cancer. Cell Commun Signal 23: 22, 2025.
40. Braicu C, Buse M, Busuioc C, Drula R, Gulei D, Raduly L, Rusu A, Irimie A, Atanasov AG, Slaby O, *et al*: A comprehensive review on MAPK: A promising therapeutic target in cancer. Cancers (Basel) 11: 1618, 2019.
41. Fang JY and Richardson BC: The MAPK signalling pathways and colorectal cancer. Lancet Oncol 6: 322-327, 2005.